

# Spin-Echo Fourier Transform Nuclear Magnetic Resonance Spectroscopy

Dallas L. Rabenstein  
and  
Thomas T. Nakashima

Department of Chemistry  
University of Alberta  
Edmonton, Alberta, Canada T6G 2G2

Pulsed Fourier transform (FT) methods for measuring high resolution nuclear magnetic resonance spectra have greatly increased the range of practical applications of NMR. Typical examples include the routine measurement of spectra for  $^{13}\text{C}$  and other isotopically dilute nuclei at the natural abundance level and the measurement of high resolution spectra for individual compounds in samples as complex as whole red blood cells.

The usual pulsed FT NMR experiment involves the application of a single, high-powered pulse of radiofrequency radiation, followed by computer acquisition of a time-domain signal, the free induction decay (FID) (1, 2). Fourier transformation of the FID yields the familiar frequency domain spectrum. State-of-the-art spectrometers also have the capability for doing multiple-pulse experiments, i.e., experiments in which a series of carefully timed pulses are applied prior to acquisition of the FID. Most such experiments were developed for the purpose of measuring relaxation times. However, with the versatility of today's spectrometers, they are being used increasingly by the NMR spectroscopist in a variety of other applications. Indeed, with today's spectrometers, the spectroscopist is often limited only by his imagination in devising multiple-pulse experiments to solve a particular problem.

Of the various multiple-pulse techniques, the spin-echo Fourier transform (SEFT) technique is one of the simplest and most useful. In its simplest form, two precisely timed pulses give rise to a spontaneous echo in the

time domain. Fourier transformation of the second half of the echo yields a frequency domain spectrum. In this article, we describe the SEFT NMR experiment and several of its applications to illustrate some of the possibilities with multiple pulse techniques.

## The SEFT NMR Experiment

Figure 1A is a schematic representation of the SEFT NMR experiment. Following the two rf pulses, there is a spontaneous echo in the time domain. The origin and shape of the echo can be accounted for in terms of the behavior of the nuclear magnetization in a rotating three-axis coordinate system (Figure 1B). The spectrometer magnetic field  $H_0$  is applied along the  $z'$  axis, and the  $x'$  and  $y'$  axes rotate around the  $z'$  axis at the spectrometer carrier frequency. Because the two possible orientations of the individual nuclear magnetic moments for spin one-half nuclei have slightly different populations and the nuclei in each orientation are randomly distributed around  $H_0$ , the ensemble of nuclei in the sample gives rise to a net macroscopic magnetization,  $M_o$ , which is colinear with and in the direction of  $H_0$ .

The component of the net magnetization projected in the  $x'y'$  plane gives rise to the NMR signal. At equilibrium, this is zero. In the pulsed NMR experiment, the system is perturbed by application of one or more rf pulses along  $x'$ , each of which will rotate  $M_o$  about the  $x'$  axis through an angle  $\alpha$  given by Equation 1

$$\alpha = \gamma H_1 t_w \quad (1)$$

$\gamma$  is the magnetogyric ratio,  $H_1$  the intensity of the magnetic component of the rf pulse, and  $t_w$  the length of the pulse (usually in the range of microseconds). In the simplest SEFT experiment, there are two pulses;  $H_1$  is the same for both pulses and  $t_w$  is changed so that the first pulse rotates  $M_o$  through  $90^\circ$  about  $x'$  and the second pulse through a further  $180^\circ$ .

Following the  $90^\circ$  pulse, the magnetization is colinear with  $y'$  (Figure 1B). This is a nonequilibrium condition, and thus the magnetization relaxes by several processes. Of interest to us here is relaxation of the component in the  $x'y'$  plane since it is this magnetization which gives the NMR signal. This component decays exponentially by spin-spin relaxation according to

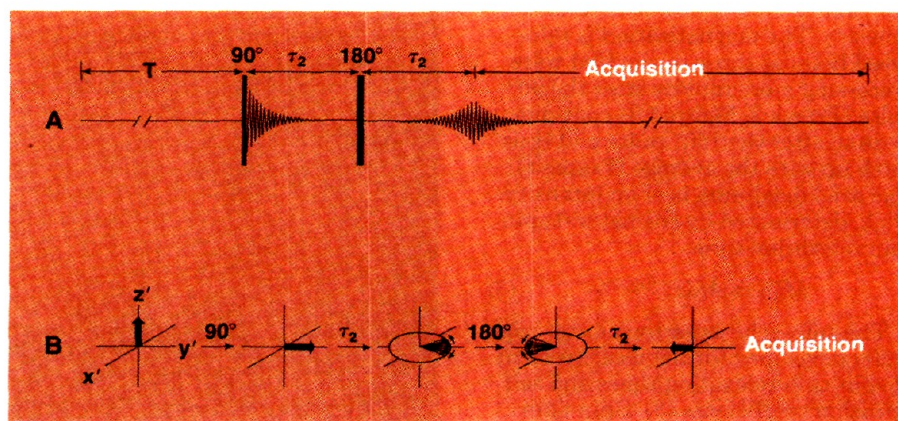
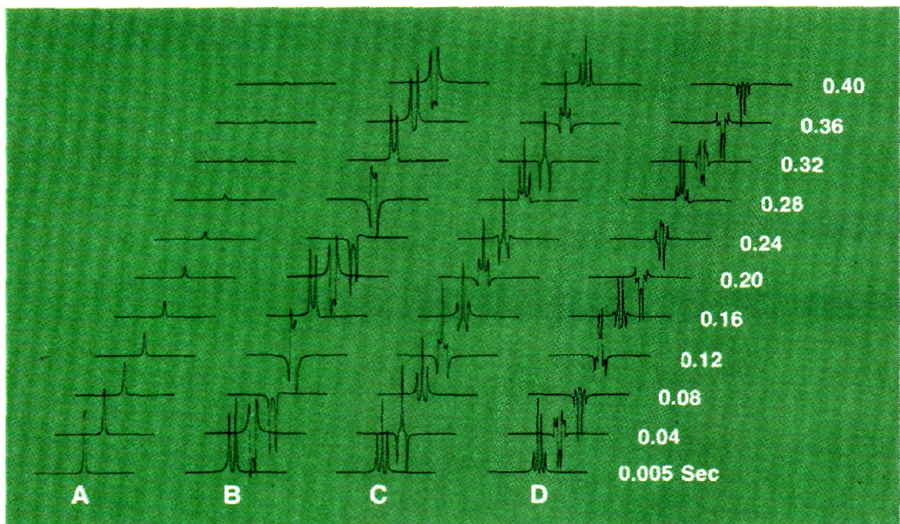


Figure 1. Schematic representations

A is the spin-echo sequence and B shows the behavior of the nuclear magnetization during the spin-echo sequence. T indicates the time before the beginning of the experiment or between successive pulse sequences



**Figure 2.** Spin-echo spectra

(A) the alcoholic proton of ethanol, (B) the methyl protons of isopropanol, (C) the methyl protons of ethanol, and (D) the methylene protons of ethanol. The times indicated are different  $\tau_2$  values in the spin-echo sequence

$$M_t^{x'y'} = M_0 e^{-t/T_2} \quad (2)$$

where  $t$  is the time following the  $90^\circ$  pulse and  $T_2$  the natural spin-spin relaxation time.

In practice, the rate of decay is generally faster than given by Equation 2 due to inhomogeneity in  $H_0$ . The effect of inhomogeneity in  $H_0$  is to cause some nuclei to precess more rapidly than the average and others to precess more slowly. Thus, the individual vectors fan out, as shown by Frame 3 in Figure 1B. This provides a second mechanism for signal decay and thus the effective  $T_2$ ,  $T_2^*$ , is a function of both the natural  $T_2$  and  $H_0$  inhomogeneity.

In the single pulse experiment, the time domain response immediately following the  $90^\circ$  pulse (Figure 1A) is the FID. In the spin-echo experiment, the  $180^\circ$  pulse is applied at time  $\tau_2$  after the  $90^\circ$  pulse to reverse the decay of  $M_{2\tau_2}^{x'y'}$  due to  $H_0$  inhomogeneity, giving rise to refocused magnetization and an echo with a maximum at time  $2\tau_2$ . The magnetization is refocused because those nuclei that were precessing more rapidly after the  $90^\circ$  pulse (Frame 3, Figure 1B) continue to do so after the  $180^\circ$  pulse and thus catch up with the average (Frame 4). The echo maximum is of an intensity,  $M_{2\tau_2}^{x'y'}$ , determined by the natural spin-spin relaxation time

$$M_{2\tau_2}^{x'y'} = M_0 e^{-2\tau_2/T_2} \quad (3)$$

The spin-echo experiment was originally developed for the measurement of spin-spin relaxation times and self-diffusion coefficients (3). Spin-spin relaxation times can be obtained directly from the magnitude of the echo as a function of  $2\tau_2$ , providing that, during the period between the  $90^\circ$

pulse and formation of the echo maximum, molecules do not diffuse to regions of the sample where  $H_0$ , and thus the precession frequency of their nuclei, are different. If such diffusion does occur, diffusion coefficients can be obtained from the decreased intensity of the echo maximum. Errors due to diffusion can be eliminated from  $T_2$  measurements by using the Carr-Purcell-Meiboom-Gill (CPMG) version of the spin-echo experiment, which makes use of a series of closely spaced  $180^\circ$  pulses following the  $90^\circ$  pulse (4, 5).

Prior to the development of pulsed FT NMR methods,  $T_2$  values were obtained from the magnitude of the echo maximum, which limited the technique to single line samples. However, Fourier transformation of the second half of the echo provides  $M_{2\tau_2}^{x'y'}$  for each of the lines in a multiline spectrum, which considerably expands the applicability of the method for measure-

ment of  $T_2$  values. The measurement of  $T_2$  values by pulsed FT NMR methods has been discussed in detail by Freeman and Hill (6).

### Phase Modulation in the SEFT Experiment

The applications of SEFT NMR discussed in this article are based on two important features: the relative intensities of resonances in SEFT spectra are different from those in the corresponding single pulse spectra if their  $T_2$  values are different (as predicted by Equation 3), and resonances which are in multiplet patterns are phase modulated (6).

Figure 2 shows the phase modulation for several first order multiplet patterns. For example, the doublet in series B gives positive, negative and out-of-phase signals. Similarly, the outer two components of the triplet and all four components of the quartet are phase modulated. In contrast, the singlet in series A simply decreases in intensity due to  $T_2$  relaxation as  $\tau_2$  is increased.

The phase modulation results from homonuclear spin-spin coupling, and for first order multiplets, it can easily be accounted for in terms of the behavior of the nuclear magnetization during the spin-echo pulse sequence. To begin, we consider a doublet which is due to spin-spin coupling to a chemically-shifted nucleus of the same isotope. For example, the doublet in Figure 2 is due to the methyl protons of isopropanol. At equilibrium, the net macroscopic magnetization from the methyl protons is colinear with  $H_0$ . The  $90^\circ$  pulse rotates the net magnetization so that it becomes colinear with  $y'$  (Frame 1, Figure 3A). However, in contrast to a singlet, where all the nuclei precess at the same frequency after the  $90^\circ$  pulse (ignoring for the moment the effect of  $H_0$  inhomogeneity), the individual methyl protons precess at one of two frequencies, de-

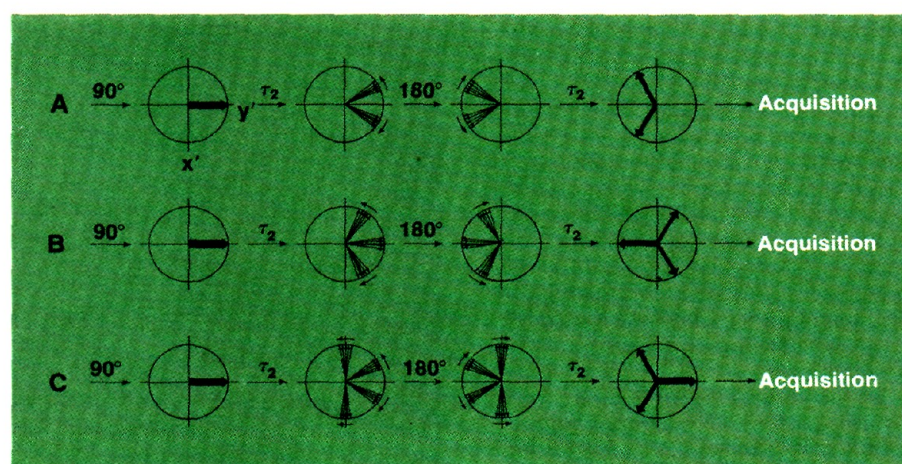


**Figure 3.** Schematic representations

The behavior of (A) doublets, (B) triplets, and (C) quartets during the spin-echo sequence

pending on the particular orientation of the methine proton to which they are coupled. The difference between the two frequencies is equal to the spin-spin coupling constant,  $J$ . For convenience, if we take the spectrometer carrier frequency to be midway between these two precession frequencies, then at time  $\tau_2$  after the  $90^\circ$  pulse, the magnetization at the two precessional frequencies is separated by a phase difference of  $(360)\tau_2J$  degrees, as shown in Frame 2 of Figure 3A. Also, the magnetization at each precessional frequency has fanned out due to  $H_0$  inhomogeneity. Application of a  $180^\circ$  pulse at time  $\tau_2$  rotates each of the sets of vectors through  $180^\circ$  around  $x'$ , which causes the fanning out due to  $H_0$  inhomogeneity to be reversed and completely eliminated at time  $2\tau_2$ . However, the separation of the two sets of vectors due to spin-spin coupling is not reversed. In fact, they continue to move further apart during the second delay period because the  $180^\circ$  pulse is a broadband pulse, i.e., all of the  $^1\text{H}$  nuclei in the sample are flipped, including the methine proton. Thus, those methyl protons which, prior to the  $180^\circ$  pulse, were coupled to a methine proton of the orientation which gave rise to the faster precessing component of the

doublet are now coupled to a methine proton of the opposite orientation. Likewise, the more slowly precessing component now becomes the faster. Consequently, rather than refocusing at time  $2\tau_2$ , the two components of the doublet are separated from each other by  $2(360)\tau_2J$  degrees. They are also out-of-phase with  $y'$ , giving rise to the phase modulation of the signals shown in Figure 2B. For example, if  $J = 6.25$  Hz, as for the methyl doublet in isopropanol, the component which was precessing more rapidly immediately following the  $90^\circ$  pulse (component A) will be  $90^\circ$  out of phase with  $y'$  when  $2\tau_2 = 0.08$  sec, ( $\tau_2 = 0.04$  sec.), the other (component B) will be  $-90^\circ$  out of phase; A and B will be  $180^\circ$  and  $-180^\circ$  out of phase, respectively, when  $2\tau_2 = 0.16$  sec,  $270^\circ$  and  $-270^\circ$  when  $2\tau_2 = 0.24$  sec, and  $360^\circ$  and  $-360^\circ$  out of phase when  $2\tau_2 = 0.32$  sec. These correspond to spectra 2-5 in Figure 2B. As  $\tau_2$  is increased further, the phase modulation cycle is repeated at a frequency of  $J$ . Thus, in general a doublet will be inverted when  $\tau_2 = 1/2J, 3/2J, 5/2J$ , etc., and positive when  $\tau_2 = 1/J, 2/J, 3/J$ , etc.

The phase modulation of triplets and quartets can be accounted for in the same way (Figures 3B and 3C). It is important to note that the central

component of a triplet is not phase modulated (Figure 2C), and that the inner and outer components of a quartet are phase modulated at different frequencies (Figure 2D). In particular, the frequency of phase modulation of the outer two components of a triplet is  $2J$ , thus they are inverted at  $\tau_2 = 1/4J, 3/4J, 5/4J$ , etc., and in phase with the central component at  $\tau_2 = 1/2J, 1/J, 3/2J$ , etc. The outer and inner components of a quartet are phase modulated at frequencies of  $3J$  and  $J$ , respectively. The outer two components will be inverted at  $\tau_2 = 1/6J, 1/2J, 5/6J$ , etc., and positive when  $\tau_2 = 1/3J, 2/3J, 1/J$ , etc., while the inner two components will be inverted at  $\tau_2 = 1/2J, 3/2J, 5/2J$ , etc., and positive when  $\tau_2 = 1/J, 2/J, 3/J$ , etc. Phase modulation of resonances in second order multiplet patterns is a more complex function of  $J$  (6).

It should be mentioned that there are several ways of circumventing  $J$  modulation in the spin-echo experiment. As described above,  $J$  modulation results when the precession frequencies of multiplet components are different during the two delay periods. This is not the case if selective  $180^\circ$  pulses are used, i.e., pulses which affect only the nuclei of interest and not those to which they are coupled, or

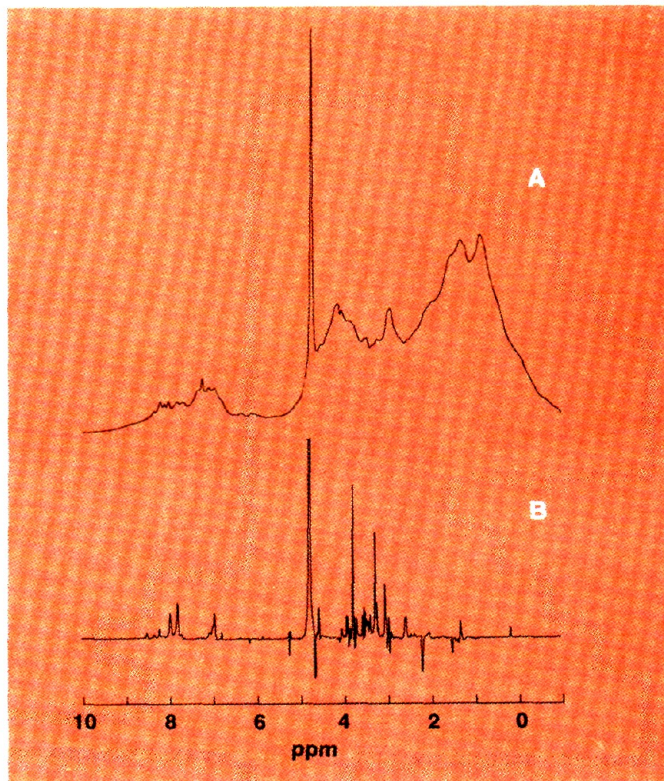


**Figure 4.** 400 MHz proton NMR spectra of red blood cells which had been washed with isotonic saline in  $\text{D}_2\text{O}$

Spectrum A is the single pulse spectrum; spectrum B is the spin-echo spectrum measured with  $\tau_2 = 0.060$  sec. Spectra were measured on a Bruker WH-400 spectrometer

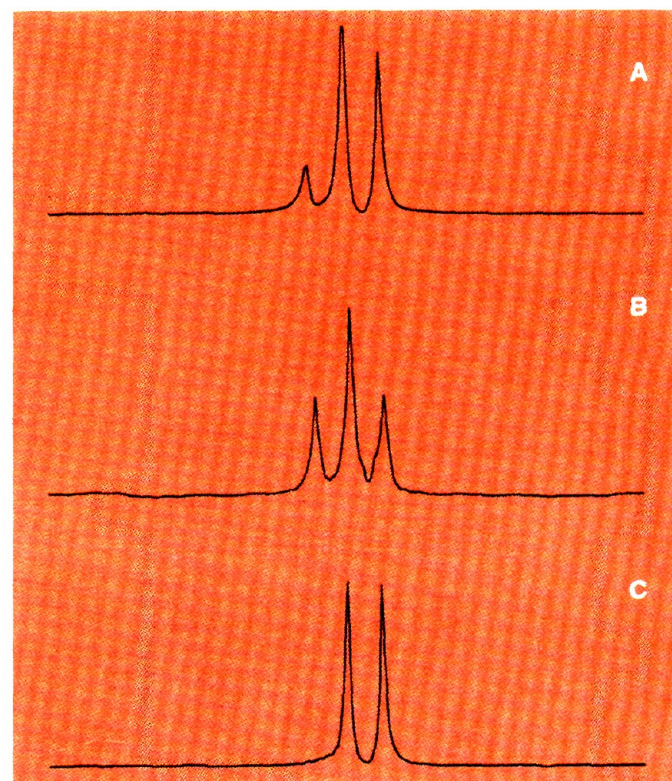


**Figure 5.** NMR spectra

Spectrum A is the methyl triplet of ethanol and the methyl doublet of *p*-isopropyl toluene. Spectra B and C are for the same sample, but were measured by the spin-echo method with gated decoupling to selectively observe the triplet and the doublet. See text for details

if nuclei are spin decoupled during the echo evolution periods. Also,  $J$  modulation is suppressed in the CPMG experiment when the  $180^\circ$  pulses are very closely spaced (6).

### Resolution Enhancement with SEFT NMR

Proton NMR spectra of large molecules and of mixtures often consist of a multitude of overlapping signals. Several methods can be used to attempt to increase the resolution, including shift reagents, spectrometers with larger magnetic fields, and multiple pulse methods. Multiple pulse methods are particularly powerful, providing increased resolution on the basis of small differences in  $T_1$  (spin-lattice relaxation time) and/or  $T_2$  values, as we described in a previous article (7), and on the basis of the phase modulation of multiplets.

The spectra in Figure 4 provide an example of the use of SEFT NMR to increase resolution based on differences in  $T_2$  values. Spectrum A is the 400 MHz single pulse  $^1\text{H}$  spectrum for red blood cells. The majority of the signals in the envelope are due to carbon-bonded protons of hemoglobin. However, because hemoglobin is a macromolecule, the  $T_2$  values for its  $^1\text{H}$  resonances are in general quite short compared to those of smaller, more mobile molecules in the red cell. Thus, by making  $\tau_2$  long enough in the spin-echo sequence, the hemoglobin resonances are eliminated from the spectrum by  $T_2$  relaxation, according to Equation 3. Spectrum B in Figure 4 is the SEFT NMR spectrum for red blood cells, measured with  $\tau_2 = 0.060$  sec. Most of the resonances in Figure 4B have been assigned to individual compounds in the red cell (8, 9).

The phase modulation of multiplet patterns can be used in several ways to enhance resolution. For example, it can sometimes be used to selectively observe one or several multiplets from a group of overlapping multiplets. To illustrate, two approaches will be described using the overlapping doublet and triplet in Figure 5A as an example. The coupling constants for these two patterns are very nearly equal, and their chemical shifts are such that the doublet overlaps with two lines of the triplet.

The most direct method for selectively observing one of the multiplet patterns makes use of gated decoupling to selectively null the other multiplet. This is accomplished by gating the decoupler on during acquisition at the chemical shift of those protons which cause the splitting of the multiplet to be nulled. For example, by gating the decoupler on during acquisition, a doublet will be converted to a singlet (Figure 6) of an intensity equal

to the sum of the intensities of the  $y'$  projection of the two lines of the doublet, i.e.,  $M_0 e^{-2\tau_2/T_2} \cos(2\pi J\tau_2)$ . The singlet is intensity modulated because it was a multiplet during evolution of the echo. Thus, the intensity of the singlet goes through a null at  $\tau_2 = 1/4J, 3/4J$ , etc. (Figure 7). Similarly, Figures 6 and 7 show that triplet and quartet patterns can be nulled through the use of selective gated decoupling. Simultaneously, phase modulation of the multiplet pattern of interest (Figure 2) can be eliminated by selectively converting it to a singlet during the evolution of the echo. Thus, the triplet in Figure 5A can be selectively observed (Figure 5B) by setting the decoupler at the chemical shift of the methylene protons of ethanol during the evolution of the echo, and then switching it to the chemical shift of the methine proton of *p*-isopropyltoluene during acquisition. The doublet can be selectively observed (Figure 5C) by simply reversing the order of the decoupler settings. When the coupling constants are nearly the same, the technique as described can be used to resolve individual patterns from overlapping doublets and triplets, overlapping triplets and quartets, and overlapping singlets and doublets, triplets or quartets. With slight modifications of the decoupling sequence, e.g., decoupling during only part of the evolution period to scale the  $J$  modulation frequencies, the technique can also be used to selectively observe overlapping multiplets of different  $J$  values.

A second method (10) for resolution enhancement based on phase modula-

tion makes use of the result that, at  $\tau_2 = 1/2J$ , doublets and quartets are inverted whereas singlets and triplets are of a positive sense (Figure 2). If the  $J$  values of the overlapping multiplets are nearly the same, or with decoupling during part of the evolution period to scale the frequency of  $J$  modulation, one can obtain multiplet subspectra consisting of singlets plus triplets or doublets plus quartets. The experiment involves measuring the single pulse spectrum and the SEFT spectrum using a  $\tau_2 = 1/2J$ . To obtain the singlet-triplet subspectrum, these two spectra are added; the doublets and the quartets are of opposite sense in the two spectra and thus they cancel. To obtain the doublet-quartet subspectra, the two spectra are subtracted.

With a little ingenuity, the spectroscopist can further modify these experiments as necessary to solve particular problems. For example, pulse sequences can be designed with which resolution can be enhanced by simultaneously taking advantage of differences in  $T_1$  and/or  $T_2$  and the nulling of interfering multiplet signals by the use of gated decoupling. We find various combinations of these techniques to be extremely powerful in our studies of individual compounds in red blood cells. As another example, by simply coupling the inversion-recovery pulse sequence for measuring spin-lattice relaxation times ( $180^\circ - \tau_1 - 90^\circ$ -acquisition) and the SEFT sequence, one has a sequence with which spin-lattice relaxation times can be measured for small molecules in solutions of macromolecules (11). The

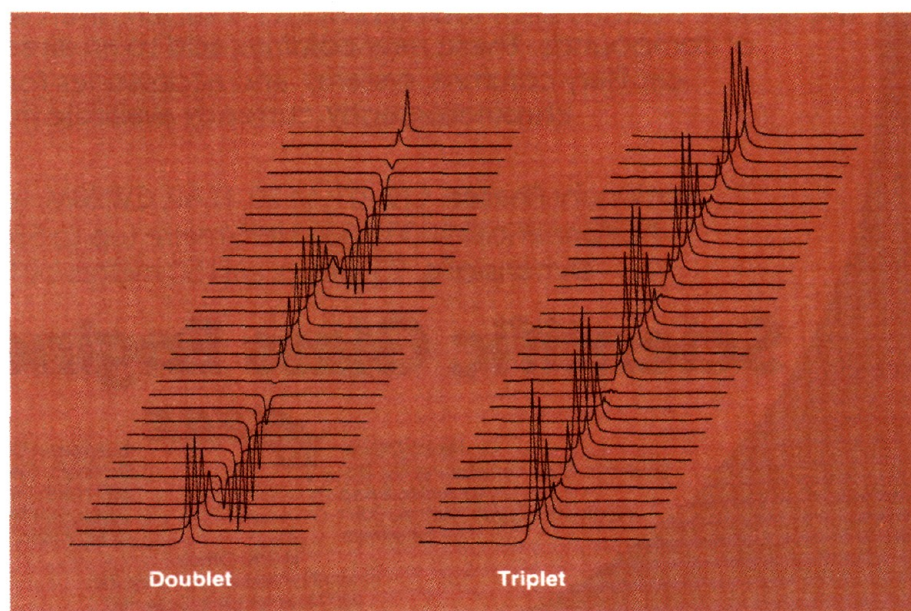


**Figure 6.** SEFT NMR spectra

Spectra measured with gated decoupling during the acquisition period for the methyl doublet of isopropanol and the methyl triplet of ethanol. The first spectrum in each series was measured with  $\tau_2 = 0.005$  sec, the second with  $\tau_2 = 0.01$  sec, and the remainder in 0.01 sec increments

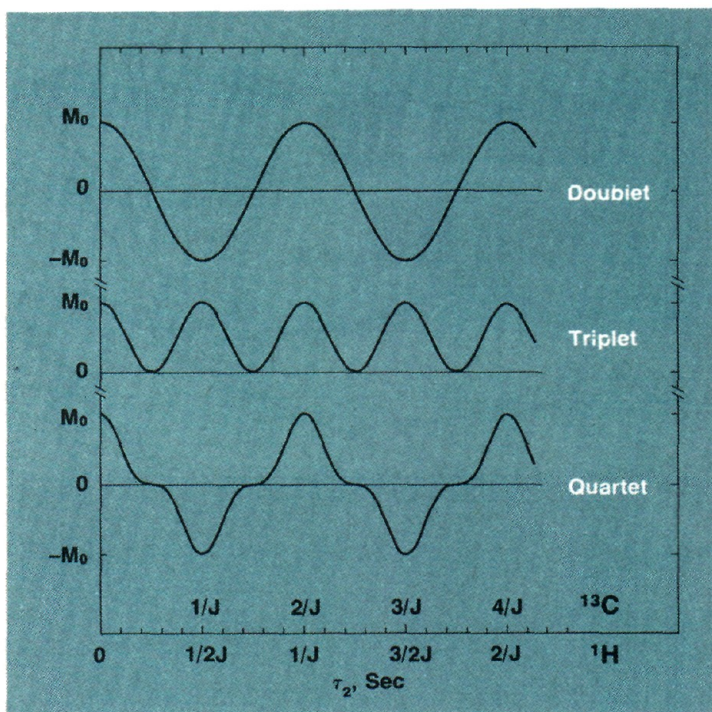


**Figure 7.** Calculated intensity modulation of SEFT spectra for doublets, triplets, and quartets

Measured by gating the decoupler on during acquisition ( $^1\text{H}$  spectra) or by gating the decoupler on during one of the delay periods and during acquisition ( $^{13}\text{C}$  spectra)

spectra in Figure 8 demonstrate the use of this combined inversion-recovery-spin-echo (IRSE) sequence to measure  $T_1$  values for individual compounds in red blood cells. These spectra also provide examples of the use of this sequence to achieve resolution enhancement on the basis of differences in both  $T_1$  and  $T_2$  values. For example, spectrum B in Figure 4 shows the enhanced resolution due to differences in  $T_2$  values; the  $\tau_1 = 0.2\text{--}1.2$  sec spectra in Figure 8 show the additional increase in resolution due to  $T_1$  differences.

#### Measurement of Unresolved Spin-Spin Coupling Constants

Spin-spin coupling constants are normally obtained directly from the separation of lines in multiplet patterns. If, however, the coupling constants are small compared with the line width, e.g., long-range couplings which are normally small or couplings in macromolecules which often have broad lines, the individual lines of a multiplet pattern are not resolved and  $J$  values cannot be measured directly. In such cases, SEFT NMR can sometimes be used to determine  $J$  values (12).

In principle,  $J$  for a doublet can be obtained from the extent of its phase modulation at a particular  $\tau_2$  value. In practice, these measurements are not very precise due to relatively small changes in signal shape with changes

in  $\tau_2$ . More precise values can be obtained through the use of gated decoupling during the acquisition period (Figure 6). For example, the singlet obtained from a doublet will go through a null at  $\tau_2 = 1/4J, 3/4J$ , etc. (Figure 7). The null point can be measured with precision from a plot of intensity vs.  $\tau_2$  at closely spaced  $\tau_2$  values. This is illustrated in Figure 9 for 2,4,5-trichlorophenol. The two aromatic protons are mutually coupled with  $J = 0.31$  Hz. Figure 9 shows the low field resonance as a function of  $\tau_2$ . The upfield part of the AX pattern was irradiated during acquisition, giving for the low field resonance a singlet which goes through a null at  $\tau_2 = 0.77$  sec from which  $J = 0.32$  Hz.

Another example of the application of this technique can be taken from our studies on red blood cells. The inverted signal at 1.46 ppm in Figure 4B is due to the methyl protons of free alanine. They are coupled to the single proton on the  $\alpha$ -carbon, giving rise to a doublet with a coupling constant of a magnitude such that the signal is inverted in the region of  $\tau_2 = 0.060$  sec. The inverted resonance does not show the doublet structure because of the large line widths, and thus the coupling constant cannot be measured directly. However, we have determined the coupling constant to be  $7.91 \pm 0.05$  Hz from the  $\tau_2$  at the null point in a series of SEFT NMR spectra measured with gated decoupling. This

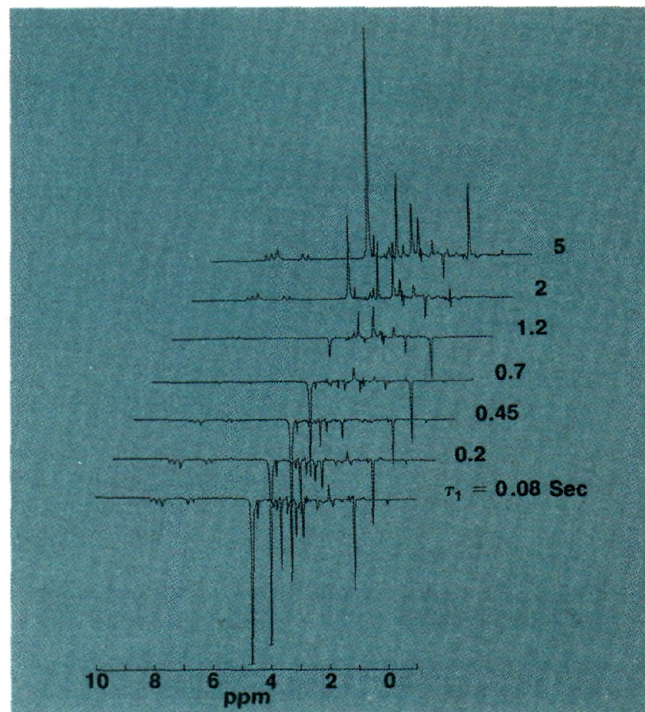


**Figure 8.** 400 MHz inversion-recovery-spin-echo ( $180^\circ-\tau_1-90^\circ-\tau_2-180^\circ-\tau_2$ -acquisition)  $^1\text{H}$  NMR spectra for red blood cells

technique has also been used to measure unresolved coupling constants in protein spectra, where again the line widths are large (12).

As a final example, we consider the use of heteronuclear spin-spin coupling in SEFT NMR spectra. NMR spectra of isotopically dilute nuclei, e.g.,  $^{13}\text{C}$ , are normally measured by the single pulse method with broadband  $^1\text{H}$  decoupling and thus they consist of singlets for each of the chemically-shifted resonances. For assignment purposes, off-resonance  $^1\text{H}$  decoupling can be used to determine the number of directly bonded protons on the carbon of a particular chemical shift. However, in some cases, the resulting  $^{13}\text{C}$  spectrum may be too complicated to analyze because of overlapping resonances. SEFT NMR techniques with gated  $^1\text{H}$  decoupling can be used in these cases.

$^{13}\text{C}$  spectra measured by the SEFT NMR method with broadband  $^1\text{H}$  decoupling throughout the experiment also consist of positive singlets. The broadband  $^1\text{H}$  decoupling eliminates any modulation from  $^1\text{H}$  coupling. The broadband  $180^\circ$  pulse at the  $^{13}\text{C}$  frequency causes no phase modulation, except in resonances from those few  $^{13}\text{C}$  nuclei which are coupled to another  $^{13}\text{C}$  nucleus, because it causes no change in spin orientation of the  $^1\text{H}$  nuclei to which the  $^{13}\text{C}$  nuclei are coupled, and thus no change in their precession frequency. However, by

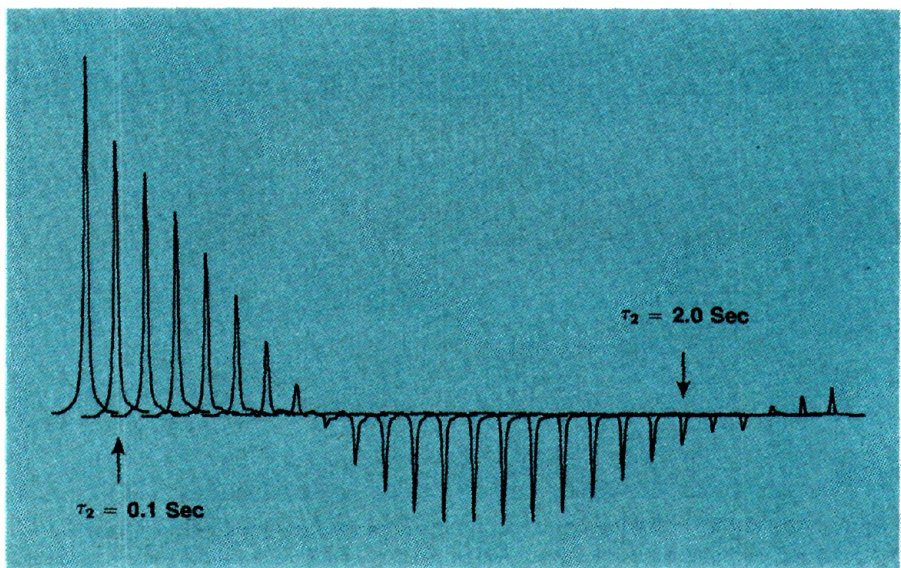


**Figure 9.** SEFT NMR spectra for the downfield aromatic proton of 2,4,5-trichlorophenol as a function of  $\tau_2$

$\tau_2$  was increased in steps of 0.1 sec. Spectra were measured with the decoupler gated on during acquisition

gating the  $^1\text{H}$  decoupler,  $^{13}\text{C}$  SEFT spectra can change in several ways. If the decoupler is on during acquisition, but off during the evolution of the echo, the spectra will also be positive singlets. In this case, the different resonances are multiplets during the evolution period; however, the precession frequencies of the different vectors are the same before and after the  $180^\circ$  pulse. Thus, prior to the  $180^\circ$  pulse the different vectors for a given  $^{13}\text{C}$  fan out, but after the pulse they refocus. If, however, the decoupler is on during just one of the two evolution periods, the different vectors will not be refocused, and the resonances will

be phase modulated (13). If in this case the decoupler is off during acquisition, the SEFT spectra will be phase modulated and will show fine structure from  $^1\text{H}$  coupling. This is illustrated in Figure 10A for benzene. If the decoupler is on during acquisition, the spectra will consist of intensity modulated singlets (Figure 10B). The details of the intensity modulation for a particular carbon will be a function of its various  $^1\text{H}$ - $^{13}\text{C}$  couplings. However, the couplings to directly bonded protons are largest and dominate the intensity modulation. Because the precession frequencies are different during only one of the two delay peri-

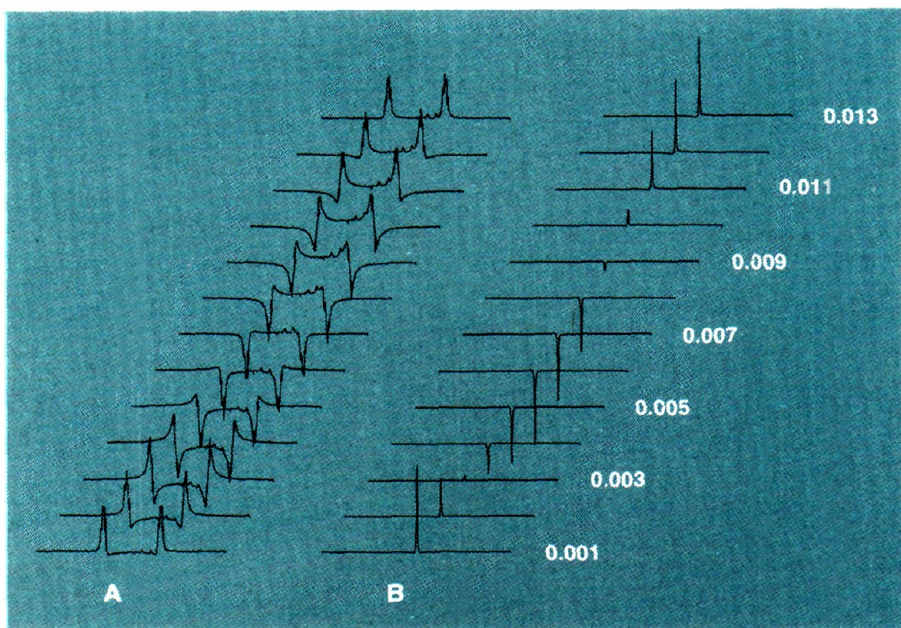


**Figure 10.**  $^{13}\text{C}$  SEFT NMR spectra for benzene

Measured (A) with the  $^1\text{H}$  broadband decoupling gated on during one of the two delay periods and (B) during one of the two delay periods and during acquisition of the FID. The  $\tau_2$  values are indicated to the right of the spectra

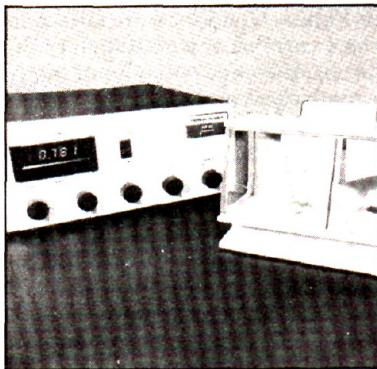
ods, the frequency of phase modulation is one-half that when the phase modulation is due to homonuclear coupling (Figure 7).

In Figure 11, spectra are shown for 3 of the 4 carbons of isobutanol, to illustrate the different behavior of methine, methylene and methyl carbons when broadband  $^1\text{H}$  decoupling is used during the first evolution period and acquisition. Over the  $\tau_2$  time scale used in Figure 11, the modulation is due almost exclusively to coupling to the directly bonded protons, and the various coupling constants can be obtained from the modulation frequencies. It also is of interest to compare the modulation behavior for the three types of carbon atoms from a qualitative point of view. The resonances from both the methine and methyl carbons go from being positive to zero to negative as  $\tau_2$  is varied; however, the  $\tau_2$  range over which the resonance intensity is near zero is much broader for the methyl carbon as compared to the methine carbon. This is because the resonance for the methine carbon is modulated at a single frequency whereas the modulation of the methyl carbon is more complex due to different modulation frequencies for the outer and inner components. This is more apparent from the predicted behavior for doublets, triplets and quartets in Figure 7. Because the intensity modulation behavior is different for these three types of carbons, each of which is also different from the behavior of a quaternary carbon, the number of directly bonded hydrogens can be determined from a series of spectra of the type shown in Figure 11. Alternatively, assignments can be made from measurements at selected  $\tau_2$  values, e.g., the spectra in Figure 11 and the calculated behavior in Figure 7 show that methine and methylene carbons or methylene and methyl carbons can easily be distinguished from a single SEFT NMR spectrum measured at  $\tau_2 = 1/4J$ . At this  $\tau_2$ , and with broadband  $^1\text{H}$  decoupling during the first evolution period and during acquisition, methine and methyl carbons will give inverted singlets, and methylene carbons will give positive singlets. Thus, the first stage of assignment can be made and coupling constants to directly bonded carbons can be obtained from a single series of SEFT spectra with gated decoupling. State-of-the-art spectrometers with their computer control of experiments can easily and efficiently be automated to carry out such measurements, e.g., in an overnight run.

### Conclusion

In this article, we have attempted to provide examples of the types of results which can be obtained with some

# Autobalance® Ultra-Microbalance



The Model AD-2Z is the latest and most advanced of three ultramicrobalances available from Perkin-Elmer. It offers unmatched weighing convenience and features not available on competitive models.

## 1. Autorange

The exclusive Autorange mode of the balance automatically selects the appropriate weighing range no matter what the sample weight and correctly positions the decimal point.

## 2. 5 Gram Capacity

The large 5 gram capacity is unique. There is no need to change the sample pan position on the beam for heavier samples. This means simple weighings with no extra manipulation of the balance.

## 3. Autozero

The Autozero switch on the Model AD-2Z can tare the full weight of any selected range, often eliminating the need for careful selection of weighing containers.

## 4. 0.1 Microgram Sensitivity

All Perkin-Elmer ultramicrobalances have a sensitivity of  $0.1\mu\text{g}$  but this is only part of the story. The Model AD-2Z is accurate to 0.01% and has a remarkable precision of  $0.05\mu\text{g}$  or better.

Circle 183 for New Brochure  
Circle 184 for Demonstration  
or call (312) 887-0770 and have  
your questions answered imme-  
diately.

You can write directly to Perkin-  
Elmer Corporation, M/S-12, Main  
Ave., Norwalk Connecticut  
06856, or Bodenseewerk Perkin-  
Elmer & Co., GmbH, Postfach  
1120, 7770 Überlingen, Federal  
Republic of Germany.

**PERKIN-ELMER**  
Responsive Technology

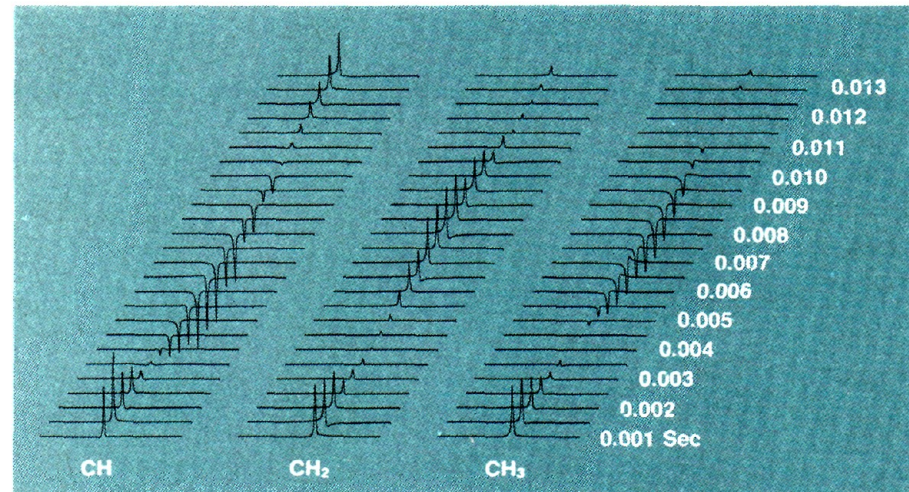


**Figure 11.**  $^{13}\text{C}$  SEFT NMR spectra for three of the four carbons of isobutanol  
Measured with the broadband  $^1\text{H}$  decoupler gated on during one of the delay periods and during acquisition

fairly simple multiple-pulse techniques. We have focused on the SEFT NMR experiment, hopefully giving enough background so that the reader can see first how the nuclear magnetization can be manipulated with carefully chosen rf pulses and gated decoupling techniques, and then how this control over the magnetization can be used in a variety of applications. It is important to emphasize that, although these experiments involve rather sophisticated sequencing

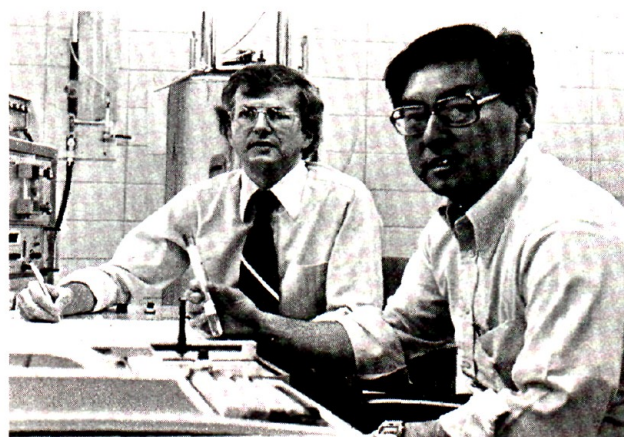
of the pulses and the gating on and off of the decoupler, and probably also changes in the decoupler frequency during the experiment, this can be accomplished rather easily with state-of-the-art spectrometers.

## Acknowledgments

It is a pleasure to acknowledge numerous discussions of the types of experiments described in this article with Anvarhusein Isab and Glen Bigam.

## References

- (1) T. C. Farrar and E. D. Becker, "Pulse and Fourier Transform NMR," Academic Press, New York, N.Y., 1971.
- (2) D. Shaw, "Fourier Transform NMR Spectroscopy," Elsevier, New York, N.Y., 1976.
- (3) E. L. Hahn, *Phys. Rev.*, **80**, 580 (1950).
- (4) H. Y. Carr and E. M. Purcell, *Phys. Rev.*, **94**, 630 (1954).
- (5) S. Meiboom and D. Gill, *Rev. Sci. Instrum.*, **29**, 688 (1958).
- (6) R. Freeman and H. D. W. Hill, in "Dynamic Nuclear Magnetic Resonance Spectroscopy," L. M. Jackman and F. A. Cotton, Eds., p 131, Academic Press, New York, N.Y., 1975.
- (7) D. L. Rabenstein, *Anal. Chem.*, **50**, 1265A (1978).
- (8) F. F. Brown, I. D. Campbell, P. W. Kuchel, and D. L. Rabenstein, *FEBS Lett.*, **82**, 12 (1977).
- (9) D. L. Rabenstein, and A. Isab, unpublished results.
- (10) I. D. Campbell, C. M. Dobson, R. J. P. Williams, and P. E. Wright, *FEBS Lett.*, **57**, 96 (1975).
- (11) D. L. Rabenstein, T. Nakashima, and G. Bigam, *J. Magn. Reson.*, **34**, 669 (1979).
- (12) I. D. Campbell, C. M. Dobson, R. G. Ratcliffe, and R. J. P. Williams, *ibid.*, **31**, 341 (1978).
- (13) G. Bodenhausen, R. Freeman, R. Niedermeyer, and D. L. Turner, *ibid.*, **26**, 133 (1977).



Dallas L. Rabenstein is a professor of chemistry and Thomas T. Nakashima is Manager of the NMR Laboratory in the Department of Chemistry of the University of Alberta.